

Airborne magnetite- and iron-rich pollution nanoparticles: potential neurotoxicants and environmental risk factors for neurodegenerative disease, including Alzheimer's disease.

Barbara A. Maher, Ph.D.

Lancaster Environment Centre, University of Lancaster

Running title: Magnetite pollution nanoparticles and AD

Centre for Environmental Magnetism & Palaeomagnetism

Lancaster Environment Centre

Lancaster University

LA1 4YQ,

UK

Tel.: (44) (0)1524 510268

Email: b.maher@lancaster.ac.uk

ABSTRACT

Fewer than 5% of Alzheimer's disease (AD) cases are demonstrably directly inherited, indicating that environmental factors may be important in initiating and/or promoting the disease. Excess iron is toxic to cells; iron overload in the AD brain may aggressively accelerate AD. Magnetite nanoparticles, capable of catalysing formation of reactive oxygen species, occur in AD plaques and tangles; they are thought to form *in situ*, from pathological iron dysfunction. A recent study has identified in frontal cortex samples the abundant presence of magnetite nanoparticles consistent with high-temperature formation; identifying therefore their external, not internal source. These magnetite particles range from ~10 to 150 nm in size, and are often associated with other, non-endogenous metals (including platinum, cadmium, cerium). Some display rounded crystal morphologies and fused surface textures, reflecting cooling and crystallization from an initially heated, iron-bearing source material. Precisely-matching magnetite 'nanospheres' occur abundantly in roadside air pollution, arising from vehicle combustion and, especially, frictional brake-wear. Airborne magnetite pollution particles < ~200 nm in size can access the brain directly via the olfactory and/or trigeminal nerves, bypassing the blood-brain barrier. Given their toxicity, abundance in roadside air, and nanoscale dimensions, traffic-derived magnetite pollution nanoparticles may constitute a chronic and pernicious neurotoxicant, and hence an environmental risk factor for AD, for large population numbers globally. Olfactory nerve damage displays strong association with AD development. Reported links between AD and occupational magnetic fields (e.g. affecting welders, machinists) may instead reflect inhalation exposure to airborne magnetic nanoparticles.

KEYWORDS: AIR POLLUTION, MAGNETITE NANOPARTICLES, ALZHEIMER DISEASE, METAL NANOPARTICLES, IRON OVERLOAD, INHALATION EXPOSURE

INTRODUCTION

Worldwide, around 36 million people are affected by Alzheimer's disease dementia, a figure expected to double in the next 20 years. Critically, fewer than 5% of AD cases are demonstrably directly inherited, indicating that environmental factors, and/or environment-gene interactions, are likely to play at least some role in initiating and/or enhancing the disease.

On a global scale, urbanisation, increasing longevity and proliferation of motor vehicle use results in chronic exposure of very large population numbers to vehicle- as well as industry-derived air pollution. Epidemiological evidence increasingly identifies the existence of associations between air pollution exposure along major traffic corridors and the incidence of neurodegenerative disease.

A recent large population study in Ontario, Canada [1] reports up to 14% increased prevalence of dementia for residents living within 50m of a major highway (hazard ratio 1.12, 95% confidence interval 1.10–1.14). In China, long-term exposure to air pollution was associated with reduced cognitive performance in verbal and numeracy tests; an association which strengthened as people aged, especially for men and the less educated [2]. Exposure to vehicle pollution increased delinquent behaviour in adolescents [3], and was associated with reduced cognitive development in children attending schools in highly polluted areas [4]. Compelling pathological evidence, in humans and animals, demonstrates that chronic exposure to particulate air pollution is associated with neuroinflammation and neurodegeneration. Brain tissue from autopsies in dogs and children living in highly polluted areas of Mexico City displayed inflammation in several brain areas [5-8].

Air pollution comprises a complex and dynamic mix of components, arising from direct emission from pollution sources, generation by atmospheric reactions, and mechanical re-suspension. Components include primary and secondary particulate matter (PM), gases, and organic compounds. Existing epidemiological evidence suggests that the PM present in polluted air represents the greatest hazard to human health.

Conventionally, mass concentrations ($\mu\text{g}/\text{m}^3$) of airborne PM have been measured (at relatively sparse, fixed monitoring stations) and reported in relation to their size (aerodynamic diameter), as this determines their degree of penetration into the body. These data have thus far formed the exposure factor in several epidemiological studies of air pollution and brain dysfunction. For example, an association was demonstrated between long-term exposure to PM_{10} (aerodynamic diameter $< 10 \mu\text{m}$) and mild cognitive impairment in elderly people [9]. Jung et al. (2015) found a 138% risk of increase of AD per increase of $4.34 \mu\text{g}/\text{m}^3$ of fine-grained PM, $\text{PM}_{2.5}$ (aerodynamic diameter $< 2.5 \mu\text{m}$) over a 9-year follow-up period in ~96,000 individuals in Taiwan [10]. Analysis of magnetic resonance imaging (MRI) data for a cohort of elderly women in the USA (the Women's Health Initiative Memory Study) showed that white matter loss was increased by 1% per $3 \mu\text{g}/\text{m}^3$ of $\text{PM}_{2.5}$ [11]. An increase in $\text{PM}_{2.5}$ of $2 \mu\text{g}/\text{m}^3$ was associated with smaller total cerebral brain volume (-0.32% , 95% confidence interval, -0.59 to -0.05) and higher odds of covert brain infarcts (1.46, 95% confidence interval, 1.10 to 1.94) [12]. Chen et al. (2017) reported an 11-year epidemiological study which found that living in places with $\text{PM}_{2.5}$ exposures higher than the Environmental Protection Agency's (EPA's) standard of $12 \mu\text{g}/\text{m}^3$ nearly doubled dementia risk in older women [13].

However, it is not yet known which properties and components of airborne PM - the particle size, particle number, composition, and/or associated chemical species - contribute most to these reported neurodegenerative effects. So far, environmental policy-makers have set targets for air pollution regulation based on the *mass* concentrations of PM ($\mu\text{g}/\text{m}^3$ of air). Notably, particles of ultrafine, nanoscale dimensions constitute by far the largest *numbers* of airborne particles to which people are exposed; such particles are, of course, so small that they contribute very little to the measured and regulated *mass* of PM. Road traffic can contribute up to 90% of the nanoparticles (NPs) in polluted urban air [14].

Nanoscale airborne particles may be a particular hazard to human health due to their reactivity (high surface to volume ratio), potential toxicity (arising from their composition and/or surface charge), and their ability to gain access to any organ, cell and organelle, including mitochondria [15]. Air pollution NPs can be internalised efficiently through inhalation and transfer via the blood circulation and/or, in the case of the brain, directly transported through the axons of the olfactory [16-18] or trigeminal nerves. Such NPs may therefore constitute a mixed group of neurotoxicants, capable of entering the brain via the olfactory system, inducing damage to the olfactory bulb (hyposmia a frequent and early indicator of neurodegenerative disease), spreading to and damaging other brain regions [19].

In animal studies, one instillation of NPs in the mouse olfactory bulb produced changes in neurotransmitter levels and pro-inflammatory cytokine mRNA expressions [20]. Mice exposed for 45 hours (over 3 weeks) to NPs collected from roadside air showed reduced cognitive function, with rapid increases of 4-hydroxy-2-nonenal (4-HNE) and 3-nitrotyrosine (3-NT) protein adducts in the olfactory bulb (OB), and increased levels of tumour necrosis factor- α (TNF α) protein in the OB, cerebral cortex and cerebellum [21]. *In vivo* and *in vitro*,

roadside NPs induced interleukin (IL)-1 α , IL-6, and TNF α , with glial responses [22].

Similarly, diesel exhaust NPs induced TNF α , IL-6, and MIP-1 α in olfactory bulb (OB) and post-olfactory brain regions [23].

Of potential key importance in neurodegeneration, iron - in oxide/hydroxide (10 - 70%), and metallic forms -, is a major and pervasive component in airborne PM in urban environments. At heavily-trafficked roadsides, iron can contribute up to ~ 6% of PM_{2.5} mass [24], but, in terms of its health impacts, its high particle number concentrations in sub-micrometer PM may be more significant. Iron-bearing NPs arise from a diverse range of emitting sources, spanning industry, domestic heating and road traffic sources. Iron-rich NPs composed of the mixed Fe²⁺/Fe³⁺ iron oxide, magnetite, have recently been found in abundance, associated with other transition and heavy metals, in the frontal cortex of post-mortem human brains [16]. In shape, size distribution and surface textures, these magnetite particles are strikingly similar to those which occur ubiquitously in air pollution at urban roadsides.

Iron in the brain: a double-edged sword

In the brain, excess levels of iron in specific brain regions are increasingly suspected of playing a major role in the pathogenesis of AD and other neurodegenerative diseases [25-29]. Iron constitutes a double-edged sword in the brain. It is an essential biometal, a component of diverse metalloproteins, from cytochromes to haemoglobin. Iron is important in myelination of neurons, and plays key roles in neuronal function, from nerve impulse transduction to neurotransmitter synthesis and mitochondrial energy production. Iron is mobilised and stored via redox cycling and valence changes, controlled by sophisticated regulatory processes of storage, transport and secretion (Fig. 1). Such processes are vital, since labile iron, i.e. in the unbound, redox-active state, can be toxic to living cells. Uncontrolled iron redox activity can

generate free radicals and other reactive oxygen species (ROS), capable of causing damage to membrane lipids, proteins and DNA in neuronal cells.

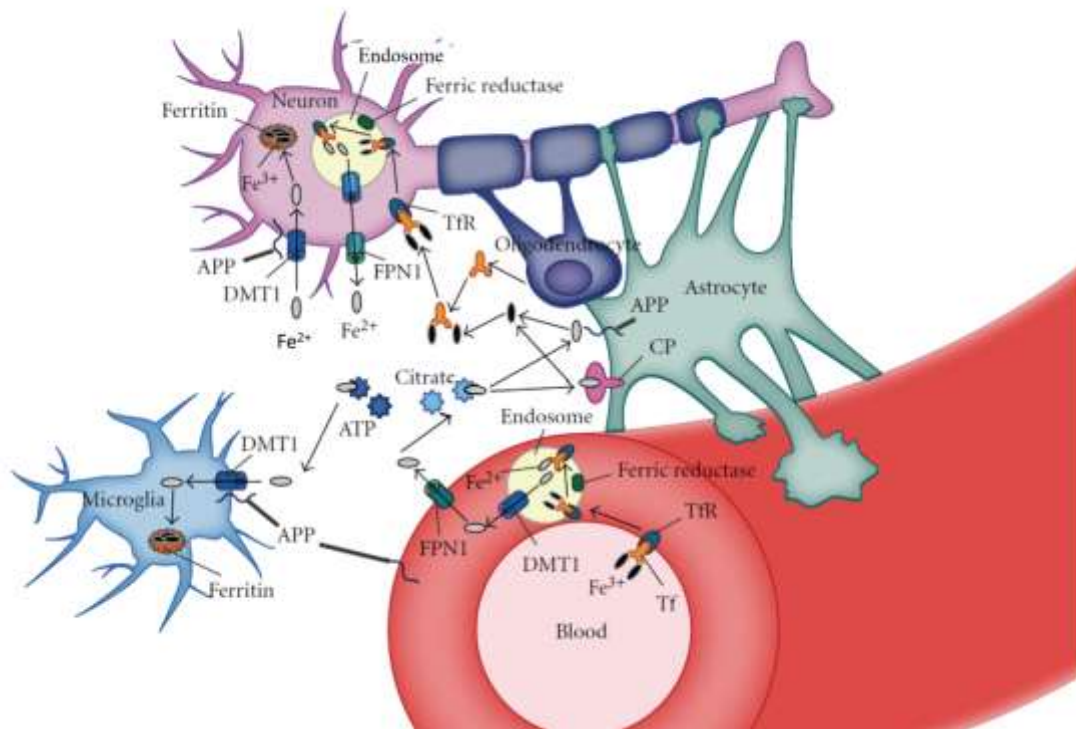


Figure 1. Iron metabolism in the brain. Iron enters the brain either bound to transferrin (Tf) or possibly unbound (especially in conditions resulting in iron overload, with transferrin saturated with iron). In the former case, Fe³⁺-laden Tf is taken up by the transferrin receptor (TfR1) in the luminal membrane of brain capillary endothelial cells and internalised in endosomes. How iron is exported from the endothelial cells is still elusive but may involve reduction to Fe²⁺, transport through the endosomal membrane by divalent metal transporter 1 (DMT1) and export into the extracellular fluid by ferroportin (FPN1). Much of the Fe²⁺ that traverses the blood-brain barrier is first oxidised, most likely by ceruloplasmin (CP) which is found in astrocytic foot processes that envelop brain endothelial cells, and then bound by Tf, synthesized by oligodendrocytes. Neurons internalize the Tf-TfR1 complex into endosomes, where iron is separated from Tf after acidification, converted into its Fe²⁺ form, and transported into the cytoplasm via DMT1 to form part of the labile iron pool. The free iron

may then be used for various cellular processes, stored as ferritin cores, or exported from the cell by FPN1. Non-transferrin-bound iron (NTBI) might be reduced by cellular reductants such as citrate or ascorbate, released by astrocytes, and then imported by oligodendrocytes and astrocytes by DMT1. Large amounts of iron, needed for axon myelination, are present in oligodendrocytes. It is less clear how glial cells acquire iron. FPN1 interacts with the amyloid precursor protein (APP), which may act as a ferroxidase at the cytoplasmic membrane of neurons, astrocytes and microglia (Adapted from [30]).

At the cellular level (Figure 1), iron homeostasis is regulated through the interactions between iron importers and exporters, iron-storage proteins, and several protein regulators, which act as sensors of iron concentrations. In the extra-cellular environment, iron is bound, as non-toxic Fe^{3+} , to the transport protein, transferrin. Iron-loaded transferrin binds to its specific receptor on the cell membrane and undergoes endocytosis. Under acidification in the endosome, the iron is released from transferrin, reduced to soluble Fe^{2+} and exported into the cytoplasm to join the labile iron pool. Iron is thus available as needed for metabolic purposes. To avoid the toxic effect of free Fe^{2+} (as below), any excess iron is oxidized (to form ferrihydrite) and sequestered into ferritin, an iron-storage protein. Because the labile iron pool is a source of redox-active iron, iron regulatory proteins (IRPs) act as iron concentration sensors, in order to control iron uptake into cells (by transferrin) and iron mineralisation and storage (by ferritin). Transferrin receptor (TfR)-mediated iron uptake and iron storage in ferritin are post-transcriptionally regulated by the IRPs. A reduction in the intracellular availability of iron causes IRPs to bind to iron response elements in the mRNAs of TfR or ferritin, thereby inhibiting translation of the mRNA of ferritin and stabilizing the mRNA of TfR. Consequently, iron unavailability leads to the reduced synthesis of ferritin and increased synthesis of TfR. Conversely, an excess of cellular iron inhibits the synthesis of TfR and

DMT1, and stimulates ferritin synthesis [31]. Together with age, iron accumulation is a risk factor for AD.

In humans, non-haem iron is stored in a relatively redox-inactive, oxidised (Fe^{3+}) form as ~8 nm spherical cores of ferrihydrite ($5\text{Fe}_2\text{O}_3 \cdot 9\text{H}_2\text{O}$) within the ~12 nm-diameter iron storage protein, ferritin. Ferritin-bound iron accumulates in different areas of the brain as it ages [32]. If redox-active, ferrous (Fe^{2+}) remains unbound and freely available, it can catalyse the formation of ROS, including the damaging hydroxyl radical ($\text{HO}\cdot$), through the Fenton reaction:



The reaction is catalytic because Fe^{3+} can then be cycled back to Fe^{2+} (Eqn 2).



Compared to cells in other tissues, the neurons, microglia and astrocytes of the brain display reduced ability to counter oxidative stress. Increased iron availability may thus pre-dispose these cells to iron-induced oxidative stress [31]. Abnormal accumulation of iron in specific regions (e.g. the substantia nigra) and pathological structures (e.g. amyloid plaques) in the brain has been shown to be associated with several different types of neurodegenerative disease, including AD, Parkinson's and Huntington's [27-29, 32]. A direct correlation between iron accumulation and amyloid plaque pathology has been reported [33-35].

Because iron oxide NPs have been targeted intensively for development for theranostic applications, their cytotoxicity has been investigated widely. Depending on their particle

size, mineral phase and, particularly, type of coating, and the diversity of cell types, exposures and assays used, superparamagnetic iron oxide nanoparticles (SPIONs) have been variously reported to induce damage to cell membranes, impaired mitochondrial function, inflammation and apoptotic responses, DNA damage, and generation of ROS, e.g. [36, 37].

For example, four different types of SPION, introduced into either C17.2 neural progenitor cells or PC12 rat pheochromocytoma cells, were all susceptible to acid-induced dissolution; resulting in release of free Fe^{2+} ions, high levels of oxidative stress and loss of cell viability [38]. Notable is that these toxic effects were removed in the presence of desferrioxamine, an iron chelator.

Magnetite and neurodegenerative disease?

Some of the excess iron found in specific locations and structures (e.g. amyloid plaques) of the neurodegenerative brain occurs in the form of magnetite, a strongly magnetic iron oxide. The presence in the brain of magnetite, a mixed $\text{Fe}^{2+}/\text{Fe}^{3+}$ iron oxide, is important because it has been directly linked with neurodegenerative disease. Fe^{2+} is highly toxic in the brain. Previous work has shown a correlation between the amount of brain magnetite and the incidence of Alzheimer's disease (AD) [39, 40]. Indeed, magnetite NPs have been found directly associated with AD senile plaques and neurofibrillary tangles [41-43].

Metal ions and their misregulation have long been suspected to play an important role in the pathogenesis of AD and other neurodegenerative diseases. Some of the key, misfolded proteins associated with these diseases (β -amyloid, α -synuclein, prion protein) have the ability to interact with redox-active metal ions, like iron (especially in its most reactive, Fe^{2+} form),

and generate ROS, including hydrogen peroxide and highly damaging hydroxyl free radicals [28, 35, 44]. Oxidative damage to brain of the type caused by ROS is a very early event in the progression of AD. *In vitro* experimental data additionally show that magnetite acts synergistically to enhance the toxicity of A β [45]. A recent *in vitro* study [46] stated that magnetite does not interact with A β , but the authors used the A β 1-16 fragment, not the full-length A β 1-42. A β 1-16 lacks the ability to aggregate into oligomers/fibrils, is not toxic and would not be expected to be redox-active.

Particulate air pollution as an external source of brain magnetite nanoparticles.

Until recently, all magnetite particles found in the human brain were assumed to be of *in situ*, biogenic origin. The distinctive, geometric, highly-crystalline brain magnetite particles originally observed (Fig. 2 A-C) by Kirschvink et al. [47], and Schultheiss-Grassi et al. [48] have been compared to the similarly ‘perfect’ magnetite crystals formed by magnetotactic bacteria (Fig. 2D-E), which seem optimised in size, and arrangement, for motile response along the Earth’s magnetic field lines [49]. The magnetic properties of magnetite particles depends on their particle size, which in turn controls their magnetic domain state, and stability. At body temperature, magnetite particles of between ~ 30 and 100 nm are magnetically single domain; such particles carry the most stable magnetizations (the only way to change the magnetization of a single domain grain is to rotate its magnetization). In contrast, magnetite particles < 30 nm in diameter are magnetically unstable at body temperature, but become stable as temperature is lowered so that thermal disordering of their magnetic moments is reduced. For example, Mössbauer and magnetic analyses of the iron-storage protein, ferritin, shows that the <~8-nm ferrihydrite-like particle cores become magnetically ordered at ~30 K [50]. In magnetotactic bacteria, the magnetite particles are

grown within pre-formed vesicles so that they achieve single domain size, and relatively uniform shapes (Fig. 2D). In the human brain, therefore, these ~30 to 100 nm, similarly geometric magnetite crystals may also be formed in order to play a specific role in a magnetic navigation sense [47, 51].

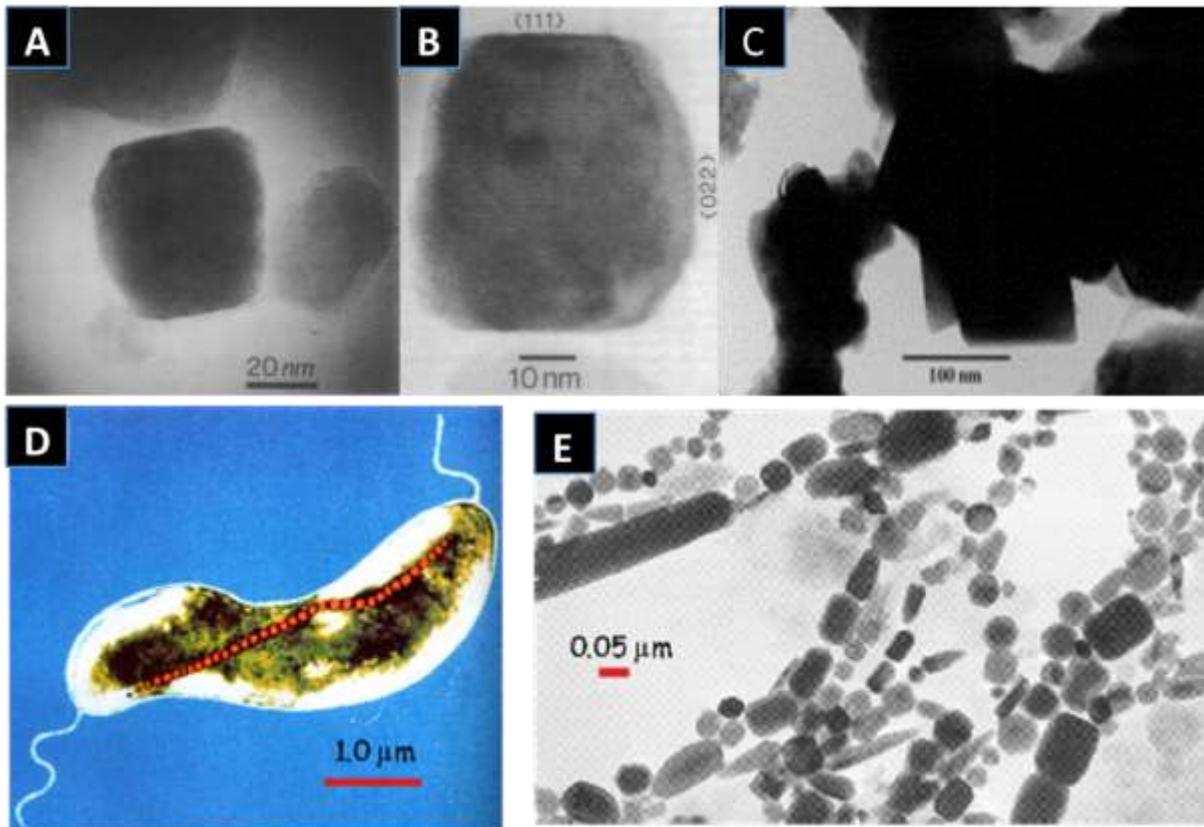


Figure 2. Magnetite particles with regular, well-formed, easily-recognized crystal faces, formed (A) to (C) in the human brain, and (D) and (E) within magnetotactic bacteria.

Transmission electron micrograph (TEM) images (A) and (B) from [47], (C) from [48], false colour scanning electron micrograph image (D) from [52], TEM image (E) from [53].

In contrast, frequently rounded magnetite crystals, of between ~ 8 and 50 nm, have been observed in association with AD plaques (Fig. 3), which have been related to dysfunctional iron metabolism [42]. These authors suggest that A β is responsible for localised accumulation of redox-active Fe²⁺, through chemical reduction of ferric (Fe³⁺) iron oxide

NPs, and iron in solution at physiological pH in the presence of aggregating A β ₁₋₄₂ [33, 34]. The ~8-nm magnetite particles these authors observe may reflect conversion of ferrihydrite within the iron-storage protein, ferritin in response to iron overload [25, 40]. Such biosynthesis of magnetite was reported recently in iron overload experiments with human stem cells. Over timescales of days, the dosed maghemite NPs were internalised and first dissolved within the cells. Subsequently, magnetite/maghemite NPs were re-formed (via the H sub-unit of ferritin), as abundant, rounded, ~8-nm particles [54]. In this study, the maghemite NPs induced slight inhibition of iron internalization (transferrin expression was down-regulated) and enhanced both iron export (ferroportin expression up-regulated) and storage (ferritin up-regulated). This biogenic formation of the strongly magnetic ferrite crystals is interpreted [54] as the cellular response to avoid long-term iron cytotoxicity. The possible suggested role of ferritin cores in aggregating [42] to form the much larger (~50 nm) spherical magnetite particles observed in some brain amyloid plaques (Fig. 3B) is an unresolved question.

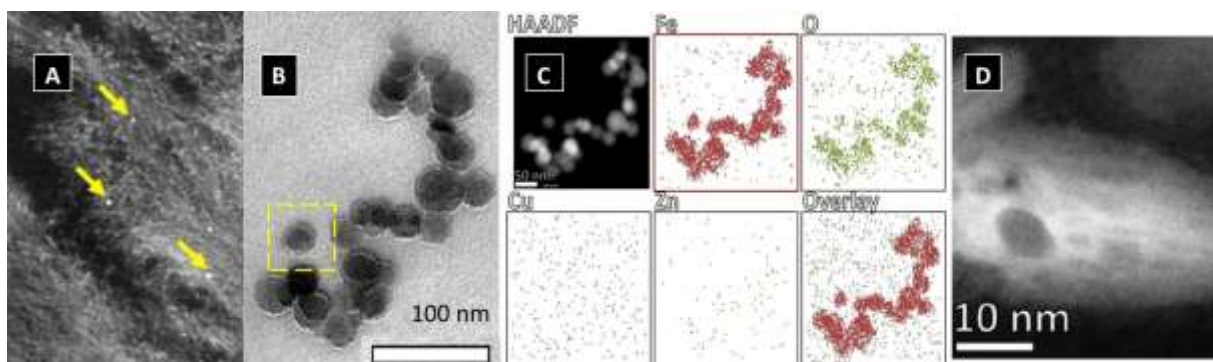


Figure 3. (A) High magnification annular dark field-scanning/transmission electron microscopy (HAADF-STEM) showing bright (electron-dense) magnetite particles (yellow arrows) associated with amyloid plaque fibres; (B) Lorentz microscopy of magnetite particles associated with the amyloid plaque; (C) Mapping of iron (Fe, red), oxygen (O, green), copper

(Cu, blue) and zinc (Zn, yellow), and overlay of iron and copper, for the magnetite particles in (B) by energy dispersive X ray analysis. (Adapted from [42]).

However, in notable addition to these reports of *endogenous* brain magnetite, a recent study [16] identified, for the first time, the abundant presence in the frontal cortex of externally-derived, magnetite pollution NPs (Figs. 4a, 5 and 6). The magnetite NPs were found in all the

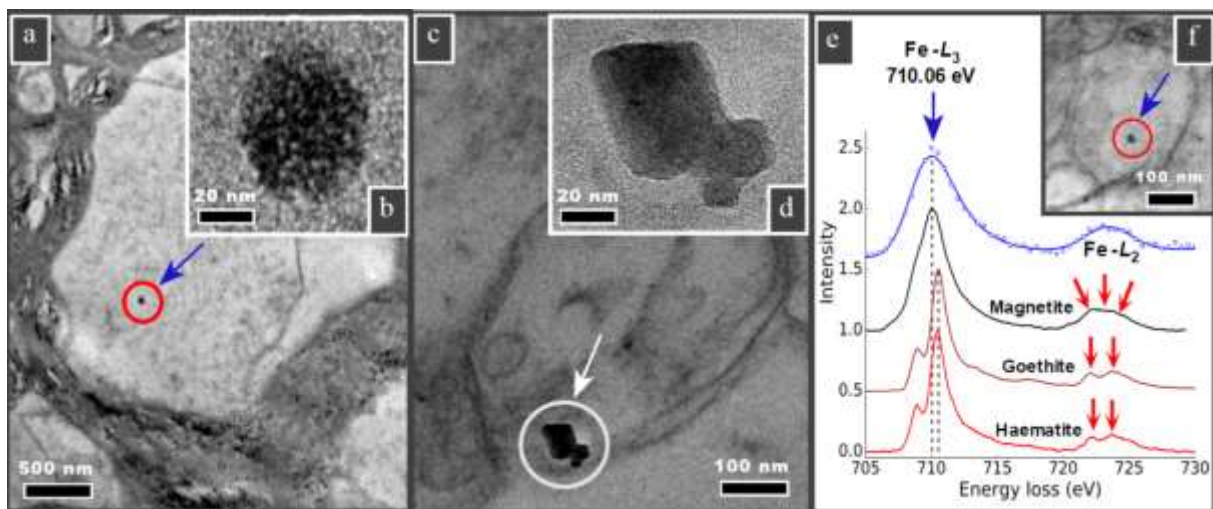


Figure 4. High resolution transmission electron micrographs of brain thin sections, showing two distinct types of magnetite NP in frontal cortex cells: (a) and (f) rounded particles, (a) shown at higher magnification in (b); and (c) angular, euhedral particles, of *in situ* formation (particles from (c) shown at higher magnification in (d)). (e) Spectroscopic analysis (electron energy loss spectroscopy, EELS), in blue for the rounded particle shown in (f), and, in black, brown and red, for standard iron oxide species. The position of the Fe–L₃ edge absorption peak, the broad feature of the Fe–L₂ (compared with the sharp edges, arrowed, of the fully oxidized Fe³⁺ phases), and the integrated areas of the L₃/L₂ (5.5) and the Fe/O (0.56) are all consistent with magnetite. (From [16]).

studied cases (i.e. from age 3 yrs upwards) but were particularly abundant in samples from older subjects (> 70 yrs at death) who had lived in Manchester, U.K. and younger subjects (~32 yrs at death) who had lived in the highly polluted atmosphere of Mexico City. In these frontal samples, two types of magnetite particles were observed. Infrequently, the highly-crystalline, geometric magnetites described by Kirschvink et al. [47] were seen (Fig. 4b). In contrast, in far greater abundance (~100 x), a second population of magnetite particles was present (Fig. 4a). These magnetite NPs displayed a wide range of particles sizes (from ~10 to 150 nm), were frequently (but not always) rounded or even spherical, and often associated with other transition metal-bearing NPs, containing, for example, Pt, Ni, Co, and Cu. They also often occurred as clusters of magnetite particles (Fig. 5).

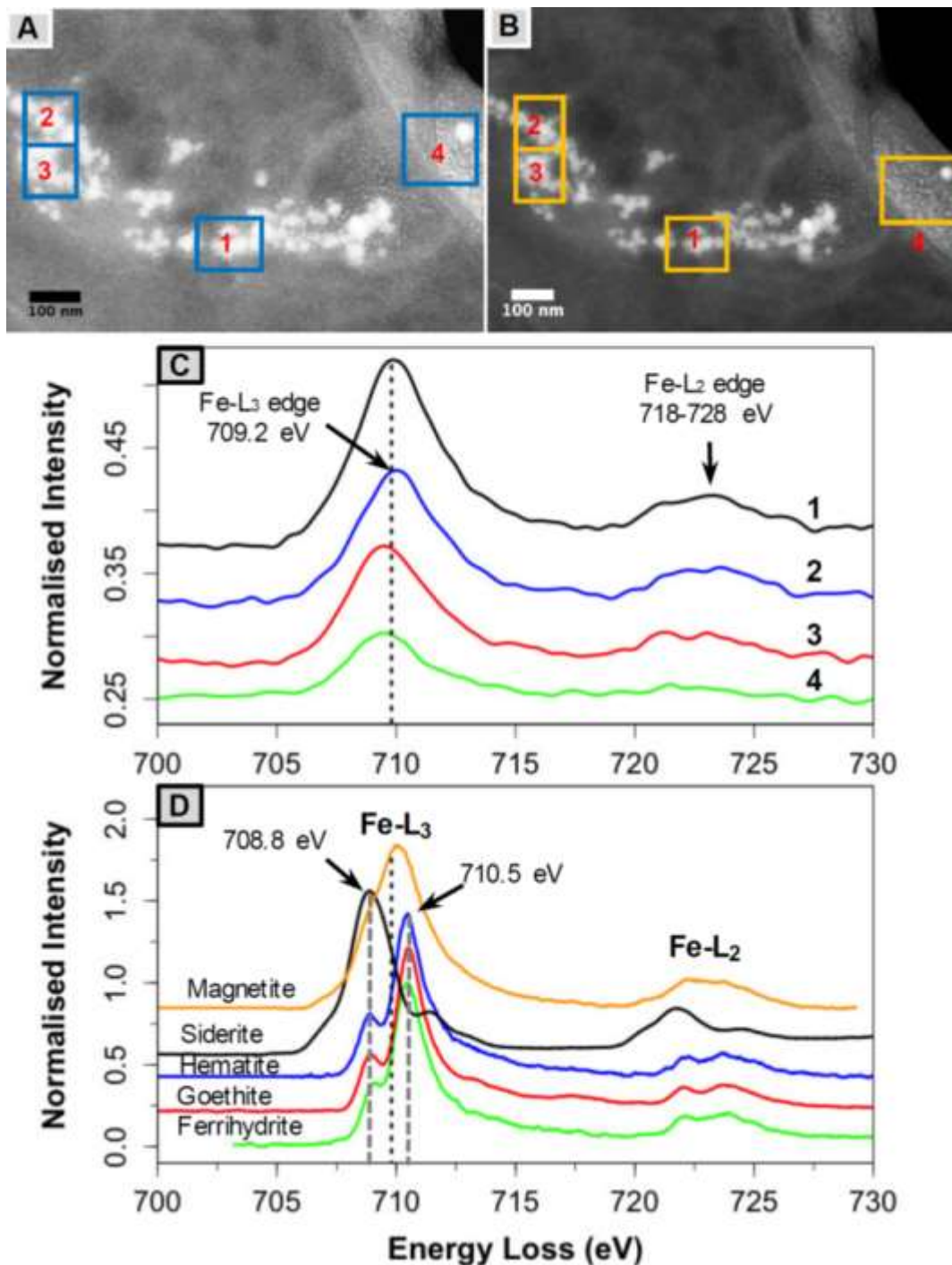


Figure 5. (A) HAADF and (B) dark-field TEM micrographs showing clusters of spherical magnetite NPs in frontal cortex samples; (C) Fe-L_{2,3} EELS spectra of nanoparticles identified in the selected areas (boxes 1-4) showing their absence of any pre-edges (see hematite, goethite and ferrihydrite pre-edge at ~708.8 eV), Fe-L₃ edges centered at 709 eV

and broad Fe- $L_{2,3}$ features characteristic of magnetite, compared with the Fe- $L_{2,3}$ EELS spectra in (D) of standard magnetite, siderite, hematite, goethite and 2-line ferrihydrite.

TEM micrographs obtained from magnetically-extracted brain magnetite NPs reveal the range of magnetite particle sizes, and the dominantly (but not exclusively) rounded/near-spherical particle shape (Fig. 6). Some of these brain magnetite particles have fused surface crystallites (Fig. 6H) that would be very difficult to reconcile with *in situ*, endogenous, low-temperature growth or dissolution formation processes.

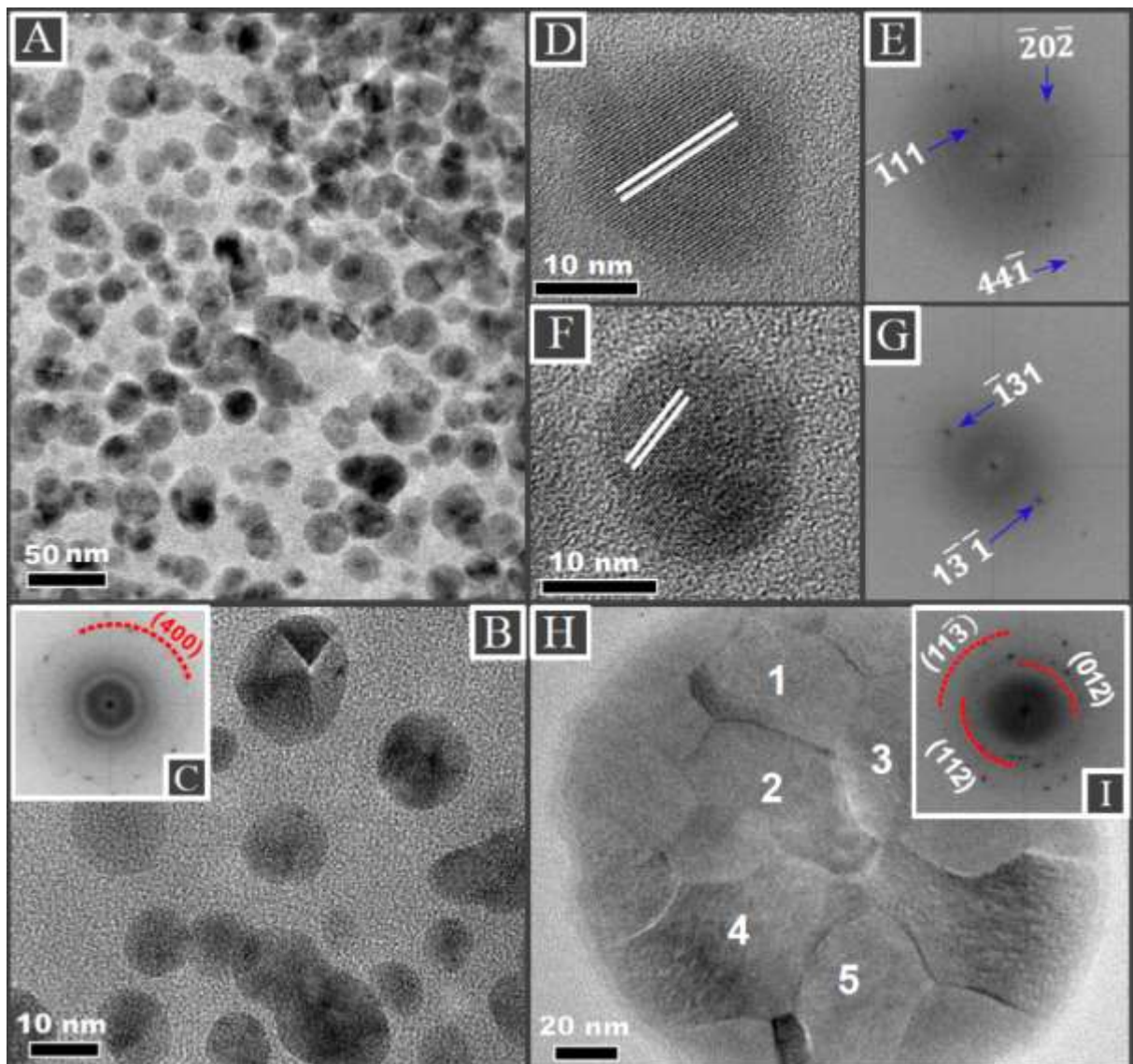


Figure 6. Transmission electron micrographs of rounded particles magnetically extracted from human brain samples: (A, D, F, and H) Mexico City cases; (B) Manchester case. (H) A large (~150-nm diameter) spherical particle with fused, interlocking magnetite/maghemite surface crystallites. (C, E, and G) Indexing of the lattice fringes of the brain particles is consistent with the (400) reflection of magnetite and (I) mixed magnetite and maghemite of selected areas 1–5 in H. (From [16]).

The concentrations of magnetite in these Manchester and Mexico City samples can be estimated from magnetic measurements (saturation remanence, at 77 K) of the tissue samples. Using a saturation remanence value of $12 \text{ Am}^2 \text{ kg}^{-1}$, for interacting, mixed single domain and superparamagnetic magnetite [55] (rather than the ‘conventional’ saturation remanence value for non-interacting, single domain magnetite, $46 \text{ Am}^2 \text{ kg}^{-1}$), magnetite concentrations in the frontal cortex samples are between 0.3 and $13.6 \mu\text{g/g}$ (dry tissue wt), and magnetite NP numbers are between 9×10^8 and $3.9 \times 10^{10}/\text{g}$ (dry tissue wt) [16].

The size distribution and surface textures of the spherical magnetite particles identified in this study, together with the co-occurrence of exogenous metal species, are all inconsistent with the characteristics of biogenically-formed magnetite [42, 47, 48]. Rather, many of them match precisely the rounded/spherical magnetite and maghemite nanoparticles (‘nanospheres’) (Fig. 7) which are both ubiquitous and abundant within air pollution: high-temperature, combustion- and friction-derived, nanoparticles (CFDNPs) (e.g. [56-61]).

The dominantly rounded shapes of the airborne, pollution-derived magnetites, and fusing of interlocking, surface crystallites reflect their high-temperature ($> \sim 200 \text{ }^\circ\text{C}$) sources, and their subsequent crystallization, upon rapid cooling and/or oxidation in the air, as iron-rich

‘nanospheres’ (Fig. 7). These iron-rich nanospheres occur as a range of iron and iron oxide phases, including strongly magnetic magnetite, and its oxidised counterpart, maghemite. In tailpipe emissions (Fig. 7A), they are formed as primary particles of incombustible ash, forming from iron impurities in fuel [59, 62, 63]), in-cylinder melting of engine fragments [58], and use of iron-rich lubricating oils and fuel additives (e.g. ferrocene) [64]. They are also formed and emitted from vehicle brake wear. Frictional heat and pressure upon braking causes the release, melting, condensation and partial oxidation of iron from the brake pad and, possibly, the brake disk.

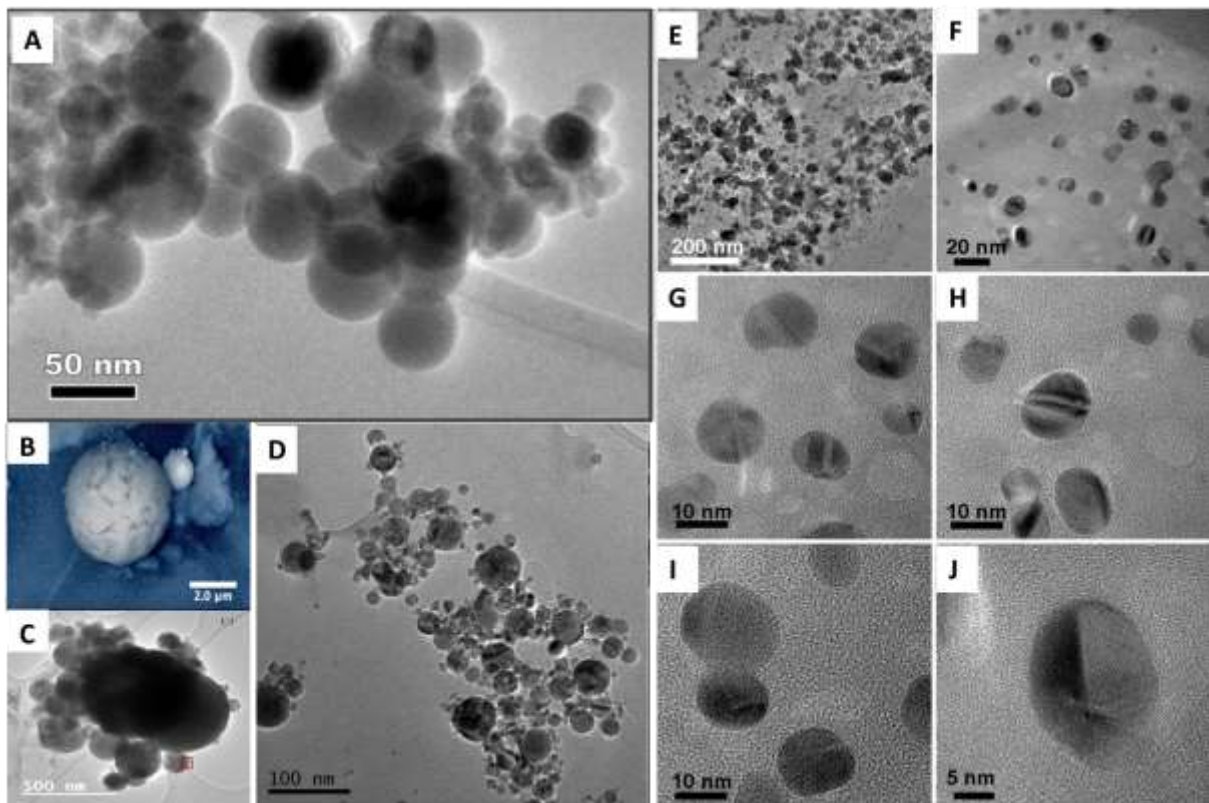


Figure 7. Magnetite and maghemite nanospheres emitted as airborne particulate pollution: (A) vehicle exhaust-derived magnetite NPs (from [58]); (B) magnetite spherule with fused surface crystallites, on a leaf surface near a power generating plant (from [16]); (C) street dust (from [65]); (D) roadside air sample, Birmingham, U.K. (from [61]); (E) – (J) roadside air samples, Lancaster, U.K. (from [16]).

Notably, in some commercially-available brake pads, up to 50% by wt magnetite powder is added as a lubricant/filler. Brake wear thus provides a substantial source of iron- and magnetite-rich NPs to the roadside air [57]. It is unsurprising that brake wear PM is orders of magnitude more magnetic than most other PM sources (Gonet & Maher, in rev.)

Sampled at a range of roadside locations, such traffic-derived magnetic NPs display a predominance of particles around 20 – 30 nm, but particles as small as ~10 nm (Fig. 7E-J) and as large as several hundred nanometres also occur (Fig. 7B; [61]). It is notable that the magnetite pollution NPs observed in human frontal cortex samples comprise a bimodal particle size distribution (Fig. 8), with one peak at ~5-10 nm (i.e. approaching ferritin-core dimensions) and a second, larger peak at ~25 nm (close to the peak particle size in airborne iron-rich NPs at the roadside).

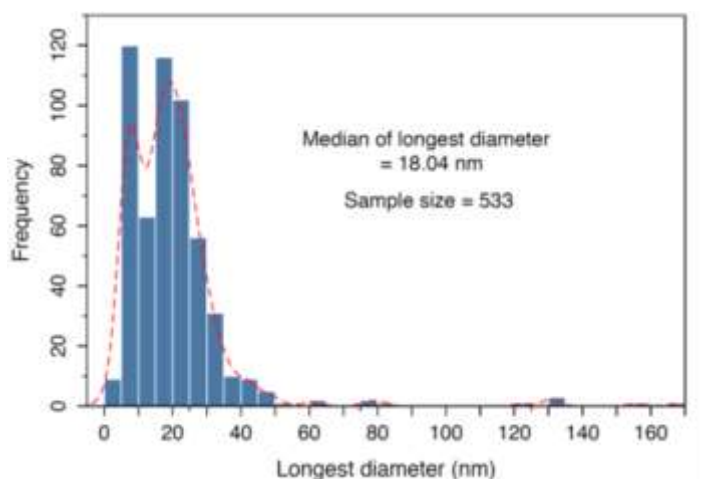


Figure 8. Particle size distribution of magnetite NPs in brain magnetic extracts from six Mexico City cases (case ID/age yrs: 282/32; 51/25; 159/26; 224/24; 146/18; 174/32), all with evolving AD pathology. ImageJ software was used to obtain the particle dimensions (from

[16]), with a measurement uncertainty of $\sim \pm 3$ to ± 5 nm, dependent on definition of individual particle edges.

Depending on PM source/s (vehicular, subway, industrial, indoor), other transition and heavy metals are often co-associated with airborne magnetite pollution nanospheres [57-61].

Magnetite NPs, containing redox-active Fe^{2+} , may be hazardous to brain health in their own right, but they also associate with other hazardous pollutants, including Mn, Pb, Zn, Li, Ba, Cr, Mn, Co and Cd and polyaromatic hydrocarbons (PAHs), including the known carcinogen, benzo[a]pyrene [66]. In the brain, evidently exogenous metals co-occur with the magnetite pollution NPs, including, for example, platinum (Mexico City case [16]) and cerium (Manchester case). These metals independently reflect transport to the brain of traffic-related air pollution, since both are increasingly prevalent due to increasing vehicular use of catalytic converters (e.g. [67]). Cerium dioxide has additionally been sold commercially (e.g. as 'Envirox') since 2004 as a diesel fuel additive [68]. Even tyre and road wear produce iron-rich NPs [69].

Thus, airborne magnetite, and other iron-rich pollution NPs, associated with transition metals and PAHs, are abundant and pervasive in the urban environment, especially along heavily-trafficked roads. For example, we have measured magnetite NP number concentrations at the roadside (in Lancaster, U.K., a relatively small city of ~142,000 people) of up to $3.8 \times 10^8/\text{m}^3$ of roadside air (for ~50 nm-sized magnetite particles, and an ambient PM_{10} concentration of ~40 $\mu\text{g}/\text{m}^3$). Magnetite NPs thus comprise ~1% of the total roadside particle numbers (much of the remainder being composed of elemental carbon and volatile organic carbon compounds) and ~10% of the primary (non-volatile) nanoparticles. Modelling studies suggest that between 0.01 and 1% of airborne NPs can be deposited in the olfactory region in humans [18]. Given a

deposition rate of 0.1% for ~20 nm particles [18], and a breathing rate of 7.5 l/min to 22 l/min, then an individual could be exposed to olfactory deposition of between ~150,000 and 500,000 magnetite NPs per hr exposure (based only on the Lancaster roadside data).

Notable too, however, is that other iron phases also occur in the urban atmosphere, depending on pollution source and degree of oxidation; including metallic iron, maghemite (the oxidised counterpart of magnetite) and the most oxidised form, haematite [61, 70]. At two roadside sites (Birmingham and Newcastle, UK), ~5% of the sub-micron Fe particles occurred as FeO, ~45% as maghemite, 35% as magnetite and the rest as haematite [61]. Because the composition of the iron-rich NP mix differs between locations and timescales (e.g. diurnal, seasonal), urban populations are likely to be exposed to differing iron oxide NP mixes.

Other sources of iron- and magnetite-rich NPs include industrial sources, including incinerators [71] and power plants [72]. Biomass burning, whether at large and episodic scale in the outdoor environment (e.g., forest fires; coal burning [72]) or for indoor heating and/or cooking purposes also supply Fe- and magnetite-rich NPs, often associated with surface-bound PAHs, some of which are carcinogenic [66]. Some candles may be a source of ferrimagnetic NPs [66].

Occupation-related exposures to sources of ultrafine iron- and magnetite-rich NPs are likely to span a rather broad range, including, for example: engine development/testing; welding [73]; machining; mechanical work; city bus driving; office exposures to some types of printer toner powders [74] [75]. Reported associations reported between AD incidence and occupation-related electromagnetic fields [76] may instead reflect increased exposure to iron-rich NPs.

DISCUSSION

A feature of global urbanisation is the proliferation of motor vehicle usage, resulting in high mass and number concentrations of roadside pollution particles. Road traffic generates abundant and pervasive Fe-rich NPs, and Fe²⁺-bearing magnetite NPs specifically, especially through friction-derived brake wear and tailpipe emissions. These combustion- and friction-derived particles (CFDNPs) are characterised by their high redox capacity, surface-bound PAHs and associations with other redox-active transition metals.

Because of the vulnerability of the brain to iron overload and resultant oxidative stress, and the iron misregulation associated with misfolded proteins in neurodegenerative disorders, the frequent inhalation of magnetite, together with associated iron oxides, transition metals and the urban atmosphere of these NPs, and their associated species, it is likely that their repeated inhalation (and transport via the olfactory and trigeminal nerves, bypassing the blood-brain barrier) provides a direct and chronic access route for iron-rich, potentially redox-active NPs into the brain. The nanoscale dimensions of such particles enables them to access cells and organelles, including mitochondria [77-79].

Since safe development of theranostic uses of magnetic NPs requires understanding of their long-term intracellular fate, a great variety of studies has investigated the degradation of SPIONs in diverse biological materials [80]. Loading of SPIONs in cultured primary astrocytes led to transient ROS formation and a strong increase in ferritin levels, indicating some release of free iron, as Fe²⁺, from the NPs, despite persistence, over 7 days, of many SPIONs in cell vesicles [81]. In U937 and THP 1 cells, SPION loading caused upregulation of lysosomal cathepsin, membranous ferroportin and ferritin degradation, associated with

secretion of both pro- and anti-inflammatory cytokines [82]. A recent study identified particle size-dependent dissolution of coated maghemite NPs in human stem cells [83]. Over a period of 27 days, NPs of ~9 nm size were dissolved entirely, within endosomes, and the excess free iron sequestered by proliferation of iron-loaded ferritin (the fate of the iron-loaded ferritin was not investigated). This degradation and storage sequence was accompanied by a 2 x increase of gene expression coding light-chain ferritin (L-ferritin, involved in iron binding and nucleation) and ferroportin (involved in cellular iron export). In contrast, larger maghemite cubes (20.5 nm edges) were only partially degraded, over the month-long experimental timescale.

The nature of the interactions in the brain between externally-sourced magnetite pollution particles and the biological matrix remains to be investigated. Almost nothing is known of the nature of any biomolecular corona formed around them, the internalization of the particles into cells and organelles, the possible sites, rates and processes of their dissolution, nor of the multiple possible impacts of their charge, size, composition, and magnetic properties.

Because dissolution of at least some of the additional iron-rich, pollution NPs is probable, the particles seen in the post-mortem brain may reflect the most recent exposures prior to death.

There is as yet no dose/response relationship for such pollution particles in the brain.

Given the probability of some dissolution [54, 83], storage [54] and/or clearance [84, 85] of the extra, pollution-sourced iron in the brain, then chronic, repeated exposure to these external sources may induce repeated, albeit transient, release of free ferrous iron, with consequent risk of oxidative stress, microgliosis, and neuronal cell death, hallmark features of neurodegenerative disease. Accumulation of redox-active iron in cerebellar glial cells has

been noted in pre-clinical AD patients, which increased as patients became progressively cognitively impaired [27]. Repeated activation of microglial responses to excess iron can induce a pro-inflammatory cycle, through increased release of cytokines and initiation of a reinforcing cycle of neuroinflammation, demyelination and neuronal damage and ferroptosis. Release of Fe^{2+} and Fe^{3+} upon cellular uptake and degradation of the iron-rich pollution NPs could drive an acceleration of the Fenton reaction, resulting in cycles of ROS formation, lipid peroxidation and misregulated neuronal death. Indeed, the efficacy of iron oxide NPs in accelerating ROS production and ferroptosis forms the basis for ferroptosis therapy in the treatment of some brain tumours [86].

Given the associations between magnetic pollution NPs and surface-bound PAHs, intense exposure to such NPs might result in evolution of pathogenesis from chronic neurodegeneration to carcinogenesis, arising from repeated damage to DNA and frequently-replenished iron supply [87].

Finally, the presence of strongly magnetic NPs in the brain might provide a means of cell damage through magnetic field-induced hyperthermia, and/or from magneto-mechanical movement of cell walls and organelles [88] and disruption of membrane gateways [47].

CONCLUSION

Of the mix of components which contribute to airborne particulate pollution, magnetite and associated Fe- and metal-rich, redox-active nanoparticles may represent a key neurotoxicant. Hence, exposure to such NPs from road traffic and other emitting sources may be an environmental risk factor for neurodegenerative disease, including Alzheimer's disease.

Conflict of Interest/Disclosure Statement

The author receives a research grant from JaguarLandRover.

REFERENCES

- [1] Chen H, Kwong JC, Copes R, Tu K, Villeneuve PJ, van Donkelaar A, Hystad P, Martin RV, Murray BJ, Jessiman B (2017) Living near major roads and the incidence of dementia, Parkinson's disease, and multiple sclerosis: a population-based cohort study. *Lancet*.
- [2] Zhang X, Chen X, Zhang X (2018) The impact of exposure to air pollution on cognitive performance. *Proc Natl Acad Sci* **115**, 9193-9197.
- [3] Younan D, Tuvblad C, Franklin M, Lurmann F, Li L, Wu J, Berhane K, Baker LA, Chen J-C (2018) Longitudinal analysis of particulate air pollutants and adolescent delinquent behavior in Southern California. *J Abnorm Child Psychol* **46**, 1283-1293.
- [4] Sunyer J, Esnaola M, Alvarez-Pedrerol M, Fornes J, Rivas I, Lopez-Vicente M, Suades-Gonzalez E, Foraster M, Garcia-Esteban R, Basagana X, Viana M, Cirach M, Moreno T, Alastuey A, Sebastian-Galles N, Nieuwenhuijsen M, Querol X (2015) Association between traffic-related air pollution in schools and cognitive development in primary school children: a prospective cohort study. *PLoS Med.* **12**, 24.
- [5] Calderon-Garciduenas L, Azzarelli B, Acuna H, Garcia R, Gambling TM, Osnaya N, Monroy S, Tizapantzi MD, Carson JL, Villarreal-Calderon A, Rewcastle B (2002) Air pollution and brain damage. *Toxicol Pathol* **30**, 373-389.
- [6] Calderon-Garciduenas L, Maronpot RR, Torres-Jardon R, Henriquez-Roldan C, Schoonhoven R, Acuna-Ayala H, Villarreal-Calderon A, Nakamura J, Fernando R, Reed W (2003) DNA damage in nasal and brain tissues of canines exposed to air pollutants is associated with evidence of chronic brain inflammation and neurodegeneration. *Toxicol. Pathol.* **31**, 524-538.
- [7] Block ML, Calderón-Garcidueñas L (2009) Air pollution: mechanisms of neuroinflammation and CNS disease. *Trends Neurosci* **32**, 506-516.
- [8] Block ML, Elder A, Auten RL, Bilbo SD, Chen HL, Chen JC, Cory-Slechta DA, Costa D, Diaz-Sanchez D, Dorman DC, Gold DR, Gray K, Jeng HA, Kaufman JD, Kleinman MT, Kirshner A, Lawler C, Miller DS, Nadadur SS, Ritz B, Semmens EO, Tonelli LH, Veronesi B, Wright RO, Wright RJ (2012) The outdoor air pollution and brain health workshop. *Neurotoxicology* **33**, 972-984.
- [9] Ranft U, Schikowski T, Sugiri D, Krutmann J, Kramer U (2009) Long-term exposure to traffic-related particulate matter impairs cognitive function in the elderly. *Environ Res* **109**, 1004-1011.
- [10] Jung C-R, Lin Y-T, Hwang B-F (2015) Ozone, particulate matter, and newly diagnosed Alzheimer's disease: a population-based cohort study in taiwan. *J Alzheimers Dis* **44**, 573-584.
- [11] Chen JC, Wang X, Wellenius GA, Serre ML, Driscoll I, Casanova R, McArdle JJ, Manson JE, Chui HC, Espeland MA (2015) Ambient air pollution and neurotoxicity on brain structure: evidence from women's health initiative memory study. *Ann Neurol* **78**, 466-476.
- [12] Wilker EH, Preis SR, Beiser AS, Wolf PA, Au R, Kloog I, Li W, Schwartz J, Koutrakis P, DeCarli C (2015) Long-term exposure to fine particulate matter, residential proximity to major roads and measures of brain structure. *Stroke* **46**, 1161-1166.
- [13] Chen H, Kwong JC, Copes R, Hystad P, van Donkelaar A, Tu KR, Brook JR, Goldberg MS, Martin RV, Murray BJ, Wilton AS, Kopp A, Burnett RT (2017) Exposure to ambient air pollution and the incidence of dementia: A population-based cohort study. *Environ Int* **108**, 271-277.
- [14] Johansson C, Norman M, Gidhagen L (2007) Spatial & temporal variations of PM10 and particle number concentrations in urban air. *Environ Monit Assess* **127**, 477-487.
- [15] Li N, Sioutas C, Cho A, Schmitz D, Misra C, Sempf J, Wang MY, Oberley T, Froines J, Nel A (2003) Ultrafine particulate pollutants induce oxidative stress and mitochondrial damage. *Environ Health Perspect* **111**, 455-460.

- [16] Maher BA, Ahmed IA, Karloukovski V, MacLaren DA, Foulds PG, Allsop D, Mann DM, Torres-Jardón R, Calderon-Garciduenas L (2016) Magnetite pollution nanoparticles in the human brain. *Proc Natl Acad Sci U S A* **113**, 10797-10801.
- [17] Oberdörster G, Sharp Z, Atudorei V, Elder A, Gelein R, Kreyling W, Cox C (2004) Translocation of inhaled ultrafine particles to the brain. *Inhal Toxicol* **16**, 437-445.
- [18] Garcia GJM, Schroeter JD, Kimbell JS (2015) Olfactory deposition of inhaled nanoparticles in humans. *Inhal Toxicol* **27**, 394-403.
- [19] Doty RL (2008) The olfactory vector hypothesis of neurodegenerative disease: Is it viable? *Ann Neurol* **63**, 7-15.
- [20] Win-Shwe TT, Mitsushima D, Yamamoto S, Fukushima A, Fujimaki H (2007) Nanoparticle induced neurotoxicity in the mice olfactory bulb: Analysis of neurotransmitter and proinflammatory cytokine mRNA levels. *Neurosci Res* **58**, S75-S75.
- [21] Cheng H, Saffari A, Sioutas C, Forman HJ, Morgan TE, Finch CE (2016) Nanoscale particulate matter from urban traffic rapidly induces oxidative stress and inflammation in olfactory epithelium with concomitant effects on brain. *Environ Health Perspect* **124**, 1537-1546.
- [22] Morgan TE, Davis DA, Iwata N, Tanner JA, Snyder D, Ning Z, Kam W, Hsu YT, Winkler JW, Chen JC, Petasis NA, Baudry M, Sioutas C, Finch CE (2011) Glutamatergic Neurons in Rodent Models Respond to Nanoscale Particulate Urban Air Pollutants in Vivo and in Vitro. *Environ Health Perspect* **119**, 1003-1009.
- [23] Levesque S, Surace MJ, McDonald J, Block ML (2011) Air pollution & the brain: Subchronic diesel exhaust exposure causes neuroinflammation and elevates early markers of neurodegenerative disease. *J Neuroinflammation* **8**, 10.
- [24] Harrison RM, Jones AM, Lawrence RG (2004) Major component composition of PM₁₀ and PM_{2.5} from roadside and urban background sites. *Atmos Environ* **38**, 4531-4538.
- [25] Castellani RJ, Moreira PI, Liu G, Dobson J, Perry G, Smith MA, Zhu X (2007) Iron: the redox-active center of oxidative stress in Alzheimer disease. *Neurochem Res* **32**, 1640-1645.
- [26] Quintana C, Bellefqih S, Laval J, Guerquin-Kern J, Wu T, Avila J, Ferrer I, Arranz R, Patino C (2006) Study of the localization of iron, ferritin, and hemosiderin in Alzheimer's disease hippocampus by analytical microscopy at the subcellular level. *J Struct Biol* **153**, 42-54.
- [27] Smith MA, Zhu XW, Tabaton M, Liu G, McKeel DW, Cohen ML, Wang XL, Siedlak SL, Dwyer BE, Hayashi T, Nakamura M, Nunomura A, Perry G (2010) Increased iron and free radical generation in preclinical Alzheimer disease and mild cognitive impairment. *J Alzheimers Dis* **19**, 363-372.
- [28] Tabner BJ, Mayes J, Allsop D (2010) Hypothesis: soluble A β oligomers in association with redox-active metal ions are the optimal generators of reactive oxygen species in Alzheimer's disease. *Int J Alzheimer's Dis* **2011**.
- [29] Hare D, Ayton S, Bush A, Lei P (2013) A delicate balance: Iron metabolism and diseases of the brain. *Front Aging Neurosci* **5**, 19.
- [30] Oshiro S, Morioka MS, Kikuchi M (2011) Dysregulation of iron metabolism in Alzheimer's disease, Parkinson's disease, and amyotrophic lateral sclerosis. *Adv Pharmacol Sci* **2011**, 378278-378278.
- [31] Crichton RR, Wilmet S, Leggsyer R, Ward RJ (2002) Molecular and cellular mechanisms of iron homeostasis and toxicity in mammalian cells. *J Inorg Biochem* **91**, 9-18.
- [32] Rouault TA (2013) Iron metabolism in the CNS: implications for neurodegenerative diseases. *Nat Rev Neurosci* **14**, 551-564.
- [33] Everett J, Cespedes E, Shelford LR, Exley C, Collingwood JF, Dobson J, van der Laan G, Jenkins CA, Arenholz E, Telling ND (2014) Ferric iron formation following the co-aggregation of ferric iron and the Alzheimer's disease peptide beta-amyloid (1-42). *J R Soc Interface* **11**, 11.
- [34] Everett J, Collingwood JF, Tjendana-Tjhin V, Brooks J, Lermyte F, Plascencia-Villa G, Hands-Portman I, Dobson J, Perry G, Telling ND (2018) Nanoscale synchrotron X-ray speciation of iron and calcium compounds in amyloid plaque cores from Alzheimer's disease subjects. *Nanoscale* **10**, 11782-11796.

- [35] Smith MA, Harris PLR, Sayre LM, Perry G (1997) Iron accumulation in Alzheimer disease is a source of redox-generated free radicals. *Proc. Natl. Acad. Sci. U. S. A.* **94**, 9866-9868.
- [36] Singh N, Jenkins GJS, Asadi R, Doak SH (2010) Potential toxicity of superparamagnetic iron oxide nanoparticles (SPION). *Nano rev* **1**.
- [37] Vogel CFA, Charrier JG, Wu DL, McFall AS, Li W, Abid A, Kennedy IM, Anastasio C (2016) Physicochemical properties of iron oxide nanoparticles that contribute to cellular ROS-dependent signaling and acellular production of hydroxyl radical. *Free Radic Res* **50**, 1153-1164.
- [38] Soenen SJH, Himmelreich U, Nuytten N, Pisanic TR, Ferrari A, De Cuyper M (2010) Intracellular nanoparticle coating stability determines nanoparticle diagnostics efficacy and cell functionality. *Small* **6**, 2136-2145.
- [39] Hautot D, Pankhurst Q, Khan N, Dobson J (2003) Preliminary evaluation of nanoscale biogenic magnetite in Alzheimer's disease brain tissue. *Proc R Soc Lond B Biol Sci* **270**, S62-S64.
- [40] Pankhurst Q, Hautot D, Khan N, Dobson J (2008) Increased levels of magnetic iron compounds in Alzheimer's disease. *J Alzheimers Dis* **13**, 49-52.
- [41] Collingwood J, Dobson J (2006) Mapping and characterization of iron compounds in Alzheimer's tissue. *J Alzheimers Dis* **10**, 215-222.
- [42] Plascencia-Villa G, Ponce A, Collingwood JF, Arellano-Jiménez MJ, Zhu X, Rogers JT, Betancourt I, José-Yacamán M, Perry G (2016) High-resolution analytical imaging and electron holography of magnetite particles in amyloid cores of Alzheimer's disease. *Sci Rep* **6**.
- [43] Telling ND, Everett J, Collingwood JF, Dobson J, van der Laan G, Gallagher JJ, Wang J, Hitchcock AP (2017) Iron biochemistry is correlated with amyloid plaque morphology in an established mouse model of Alzheimer's disease. *Cell Chem Biol* **24**, 1205-+.
- [44] Allsop D, Mayes J, Moore S, Masad A, Tabner BJ (2008) Metal-dependent generation of reactive oxygen species from amyloid proteins implicated in neurodegenerative disease. *Biochem Soc Trans* **36**, 1293-1298.
- [45] Teller S, Tahirbegi IB, Mir M, Samitier J, Soriano J (2015) Magnetite-Amyloid-beta deteriorates activity and functional organization in an in vitro model for Alzheimer's disease. *Sci Rep* **5**.
- [46] Gumpelmayer M, Nguyen M, Molnar G, Bousseksou A, Meunier B, Robert A (2018) Magnetite Fe₃O₄ has no intrinsic peroxidase activity, and is probably not involved in Alzheimer's oxidative stress. *Angew Chem Int Ed* **57**, 14758-14763.
- [47] Kirschvink JL, Kobayashi-Kirschvink A, Woodford BJ (1992) Magnetite biomineralization in the human brain. *Proc Natl Acad Sci U. S. A.* **89**, 7683-7687.
- [48] Schultheiss-Grassi PP, Wessiken R, Dobson J (1999) TEM investigations of biogenic magnetite extracted from the human hippocampus. *Biochim Biophys Acta* **1426**, 212-216.
- [49] Lefevre CT, Bazylinski DA (2013) Ecology, diversity, and evolution of magnetotactic bacteria. *Microbiol Mol Biol Rev* **77**, 497-526.
- [50] StPierre TG, Chan P, Bauchspiess KR, Webb J, Betteridge S, Walton S, Dickson DPE (1996) Synthesis, structure and magnetic properties of ferritin cores with varying composition and degrees of structural order: Models for iron oxide deposits in iron-overload diseases. *Coord Chem Rev* **151**, 125-143.
- [51] Wang CX, Hilburn IA, Wu D-A, Mizuhara Y, Cousté CP, Abrahams JNH, Bernstein SE, Matani A, Shimojo S, Kirschvink JL (2019) Transduction of the geomagnetic field as evidenced from alpha-band activity in the human brain. *eneuro*.0483-0418.2019.
- [52] Petersen N, Vondobeneck T, Vali H (1986) Fossil bacterial magnetite in deep-sea sediments from the South Atlantic Ocean. *Nature* **320**, 611-615.
- [53] Maher BA, Thompson, R. (1999) *Quaternary Climates, Environments and Magnetism*, CUP.
- [54] Van de Walle A, Plan Sangnier A, Abou-Hassan A, Curcio A, Hemadi M, Menguy N, Lalatonne Y, Luciani N, Wilhelm C (2019) Biosynthesis of magnetic nanoparticles from nano-degradation products revealed in human stem cells. *Proc Natl Acad Sci U. S. A.*

- [55] Maher BA (1988) Magnetic properties of some synthetic sub-micron magnetites. *Geophys J Int* **94**, 83-96.
- [56] Chen Y, Shah N, Huggins FE, Huffman GP (2006) Microanalysis of ambient particles from Lexington, KY, by electron microscopy. *Atmos Environ* **40**, 651-663.
- [57] Kukutschova J, Moravec P, Tomasek V, Matejka V, Smolik J, Schwarz J, Seidlerova J, Safarova K, Filip P (2011) On airborne nano/micro-sized wear particles released from low-metallic automotive brakes. *Environ Pollut* **159**, 998-1006.
- [58] Liati A, Pandurangi SS, Boulouchos K, Schreiber D, Dasilva YAR (2015) Metal nanoparticles in diesel exhaust derived by in-cylinder melting of detached engine fragments. *Atmos Environ* **101**, 34-40.
- [59] Mitchell R, Maher BA (2009) Evaluation and application of biomagnetic monitoring of traffic-derived particulate pollution. *Atmos Environ* **43**, 2095-2103.
- [60] Moreno T, Martins V, Querol X, Jones T, Berube K, Minguillon MC, Amato F, Capdevila M, de Miguel E, Centelles S, Gibbons W (2015) A new look at inhalable metalliferous airborne particles on rail subway platforms. *Sci Total Environ* **505**, 367-375.
- [61] Sanderson P, Su S, Chang I, Saborit JD, Kepaptsoglou D, Weber R, Harrison RM (2016) Characterisation of iron-rich atmospheric submicrometre particles in the roadside environment. *Atmos Environ* **140**, 167-175.
- [62] Abdul-Razzaq W, Gautam M (2001) Discovery of magnetite in the exhausted material from a diesel engine. *Appl Phys Lett* **78**, 2018-2019.
- [63] Matzka J, Maher BA (1999) Magnetic biomonitoring of roadside tree leaves: identification of spatial and temporal variations in vehicle-derived particulates. *Atmos Environ* **33**, 4565-4569.
- [64] Lee D, Miller A, Kittelson D, Zachariah MR (2006) Characterization of metal-bearing diesel nanoparticles using single-particle mass spectrometry. *J Aerosol Sci* **37**, 88-110.
- [65] Yang Y, Vance M, Tou F, Tiwari A, Liu M, Hochella MF, Jr. (2016) Nanoparticles in road dust from impervious urban surfaces: distribution, identification, and environmental implications. *Environ Sci-Nano* **3**, 534-544.
- [66] Halsall CJ, Maher BA, Karloukovski VV, Shah P, Watkins SJ (2008) A novel approach to investigating indoor/outdoor pollution links: Combined magnetic and PAH measurements. *Atmos Environ* **42**, 8902-8909.
- [67] Gomez B, Gomez M, Sanchez J, Fernandez R, Palacios M (2001) Platinum and rhodium distribution in airborne particulate matter and road dust. *Sci Total Environ* **269**, 131-144.
- [68] Wakefield G, Wu X, Gardener M, Park B, Anderson S (2008) Envirox fuel-borne catalyst: Developing and launching a nano-fuel additive. *Technol Anal Strateg Manag* **20**, 127-136.
- [69] Gustafsson M, Blomquist G, Gudmundsson A, Dahl A, Swietlicki E, Bohyard M, Lindbom J, Ljungman A (2008) Properties and toxicological effects of particles from the interaction between tyres, road pavement and winter traction material. *Sci Total Environ* **393**, 226-240.
- [70] Hansard R, Maher BA, Kinnersley RP (2012) Rapid magnetic biomonitoring and differentiation of atmospheric particulate pollutants at the roadside and around two major industrial sites in the UK. *Environ Sci Technol* **46**, 4403-4410.
- [71] Funari V, Mantovani L, Vigliotti L, Tribaudino M, Dinelli E, Braga R (2018) Superparamagnetic iron oxides nanoparticles from municipal solid waste incinerators. *Sci Total Environ* **621**, 687-696.
- [72] Sehn JL, de Leao FB, da Boit K, Oliveira MLS, Hidalgo GE, Sampaio CH, Silva LFO (2016) Nanomineralogy in the real world: A perspective on nanoparticles in the environmental impacts of coal fire. *Chemosphere* **147**, 439-443.
- [73] Jenkins NT, Eagar TW (2005) Chemical analysis of welding fume particles - Airborne particle size is the most important factor in determining the accuracy of a method for chemical analysis. *Weld J* **84**, 87S-93S.
- [74] Zhang Y, Demokritou P, Ryan DK, Bello D (2019) Comprehensive Assessment of Short-Lived ROS and H₂O₂ in Laser Printer Emissions: Assessing the Relative Contribution of Metal Oxides and Organic Constituents. *Environ Sci Technol*

- [75] Könczöl M, Ebeling S, Goldenberg E, Treude F, Gminski R, Gieré R, Grobéty B, Rothen-Rutishauser B, Merfort I, Mersch-Sundermann V (2011) Cytotoxicity and genotoxicity of size-fractionated iron oxide (magnetite) in A549 human lung epithelial cells: role of ROS, JNK, and NF- κ B. *Chem Res Toxicol* **24**, 1460-1475.
- [76] Hakansson N, Gustavsson P, Johansen C, Floderus B (2003) Neurodegenerative diseases in welders and other workers exposed to high levels of magnetic fields. *Epidemiol* **14**, 420-426.
- [77] Park EJ, Choi DH, Kim Y, Lee EW, Song J, Cho MH, Kim JH, Kim SW (2014) Magnetic iron oxide nanoparticles induce autophagy preceding apoptosis through mitochondrial damage and ER stress in RAW264.7 cells. *Toxicol In Vitro* **28**, 1402-1412.
- [78] Zhang XD, Zhang HQ, Liang X, Zhang JX, Tao W, Zhu XB, Chang DF, Zeng XW, Mei L (2016) Iron oxide nanoparticles induce autophagosome accumulation through multiple mechanisms: lysosome impairment, mitochondrial damage, and ER stress. *Mol Pharm* **13**, 2578-2587.
- [79] Gonzalez-Maciel A, Reynoso-Robles R, Torres-Jardon R, Mukherjee PS, Calderon-Garciduenas L (2017) Combustion-derived nanoparticles in key brain target cells and organelles in young urbanites: culprit hidden in plain sight in Alzheimer's disease development. *J Alzheimers Dis* **59**, 189-208.
- [80] Soenen SJ, Parak WJ, Rejman J, Manshian B (2015) (Intra)Cellular stability of inorganic nanoparticles: Effects on cytotoxicity, particle functionality, and biomedical applications. *Chem Rev* **115**, 2109-2135.
- [81] Geppert M, Hohnholt MC, Nurnberger S, Dringen R (2012) Ferritin up-regulation and transient ROS production in cultured brain astrocytes after loading with iron oxide nanoparticles. *Acta Biomater* **8**, 3832-3839.
- [82] Laskar A, Ghosh M, Khattak SI, Li W, Yuan XM (2012) Degradation of superparamagnetic iron oxide nanoparticle-induced ferritin by lysosomal cathepsins and related immune response. *Nanomedicine* **7**, 705-717.
- [83] Mazuel F, Espinosa A, Luciani N, Reffay M, Le Borgne R, Motte L, Desboeufs K, Michel A, Pellegrino T, Lalatonne Y, Wilhelm C (2016) Massive intracellular biodegradation of iron oxide nanoparticles evidenced magnetically at single-endosome and tissue levels. *ACS Nano* **10**, 7627-7638.
- [84] Hwang FH, Kim DK, Yoshitake T, Johansson SM, Bjelke B, Muhammed M, Kehr J (2011) Diffusion and clearance of superparamagnetic iron oxide nanoparticles infused into the rat striatum studied by MRI and histochemical techniques. *Nanotechnol* **22**.
- [85] Polikarpov D, Cherepanov V, Chuev M, Gabbasov R, Mischenko I, Nikitin M, Vereshagin Y, Yurenia A, Panchenko V (2014) Mossbauer evidence of (Fe₃O₄)-Fe-57 based ferrofluid biodegradation in the brain. *Hyperfine Interact* **226**, 421-430.
- [86] Shen ZY, Liu T, Li Y, Lau J, Yang Z, Fan WP, Zhou ZJ, Shi CR, Ke CM, Bregadze VI, Mandal SK, Liu YJ, Li ZH, Xue T, Zhu GZ, Munasinghe J, Niu G, Wu AG, Chen XY (2018) Fenton-reaction-acceleratable magnetic nanoparticles for ferroptosis therapy of orthotopic brain tumors. *ACS Nano* **12**, 11355-11365.
- [87] Bystrom LM, Guzman ML, Rivella S (2014) Iron and reactive oxygen species: friends or foes of cancer cells? *Antioxid Redox Signal* **20**, 1917-1924.
- [88] Valberg PA, Feldman HA (1987) Magnetic particle motions within living cells - measurement of cytoplasmic viscosity and motile activity. *Biophys J* **52**, 551-561.